Ultrasonics Sonochemistry 82 (2022) 105903

Contents lists available at ScienceDirect

Ultrasonics Sonochemistry

journal homepage: www.elsevier.com/locate/ultson

Triple-combination therapy assisted with ultrasound-active gold nanoparticles and ultrasound therapy against 3D cisplatin-resistant ovarian cancer model

Bilgi Kip [a,b], Cansu Umran Tunc [a,b], Omer Aydin [a,b,c,d,*]

[a] Department of Biomedical Engineering, Erciyes University, Kayseri 38039, Turkey
[b] NanoThera Lab, ERFARMA-Drug Development and Implementation Center, Erciyes University, 38039 Kayseri, Turkey
[c] ERNAM-Nanotechnology Research and Application Center, Erciyes University, Kayseri 38039, Turkey
[d] ERKAM-Clinical Engineering Research and Application Center, Erciyes University, Kayseri 38040, Turkey

ARTICLE INFO

Keywords:
Ovarian cancer
Ultrasound therapy
Ultrasound-active gold nanoparticles
Cisplatin
Drug resistance
Triple combination therapy
Gold Nanocones

ABSTRACT

Cancer chemotherapy suffers from drug resistance and side effects of the drugs. Combination therapies have been attracted attention to overcome these limitations of traditional cancer treatments. Recently, increasing in intracellular chemotherapeutic concentration in the presence of ultrasonic waves (US) has been shown in the preclinical stage. In addition, some recent studies have shown that nanoparticles increase the effectiveness of ultrasound therapy. In this study, the US-active property of gold nanocones (AuNCs) was utilized for combinational US and cisplatin (Cis) to overcome drug resistance. The effect of the triple combination therapy US + AuNCs + Cis with low-dose Cis on 2/3D models of cisplatin-resistant ovarian cancer cell line (A2780cis) were investigated. In the 2D cell culture, 60% of the A2780cis cell population was suppressed with triple combination therapy; and the long-term therapeutic efficacy of the US + AuNCs + Cis with the low-dose drug was demonstrated by suppressing 83% of colony formation. According to the results in the 3D cell model, 60% of the spheroid formation was suppressed by the triple combination therapy with low-dose Cis. These results not only demonstrate the success of the US + AuNCs + Cis triple combination therapy for its long-term therapeutic effect on resistant cancer cells but also verified that it might enable effective cancer therapy in vivo and clinical stages based on the 3D tumor models. In addition, enhanced anti-cancer activity was demonstrated at the low-dose Cis on drug-resistant cancer cells indicating the triple-combination therapy successfully overcame drug resistance and this is a promising strategy to reduce the side effects of chemotherapy. This work exhibits a novel US and AuNCs-mediated combination cancer therapy, which demonstrates the role of ultrasound-active AuNCs to combat drug resistance with low-dose chemotherapy.

1. Introduction

Cancer therapies suffer from not only the nonspecific toxic effects of chemotherapeutics [1,2], but also the rapid development of chemoresistance pathways [3]. In recent years, combination cancer therapies have attracted a great deal of attention for developing of effective therapies by sensitizing cells to the drug due to the limited success of single treatments [4]. Previous preclinical studies have shown that ultrasound therapy is an effective treatment strategy to enhance the chemotherapeutic effect; therefore, the combination of US and chemotherapy shows promise in overcoming drug resistance [5–7]. In the presence of US therapy, the porosity of the cell membrane increases due to the mechanical effect [8]. It also has advantages over other clinical treatments used in cancer therapy such as photothermal therapy [9] and radiation therapy [10] since it is non-invasive, has high tissue penetration, and the acoustic wave does not cause systemic toxicity [11]. In addition to these advantages of US therapy, it offers a definite innovative and important new perspectives in cancer treatment such as an increased therapeutic concentration in the tumor [12], immunomodulating effects [13], and different focused ultrasound therapy modalities [14,15]. The combination therapy of US and chemotherapy increases the drug accumulation in the tumor cells. Thus, this combination therapy can combat various resistance mechanisms that have developed against chemotherapeutics [16]. For instance; Cao et al. showed that the

* Corresponding author at: Department of Biomedical Engineering, Erciyes University, Kayseri 38039, Turkey.
E-mail address: biomer@umich.edu (O. Aydin).

https://doi.org/10.1016/j.ultsonch.2021.105903
Received 8 November 2021; Received in revised form 17 December 2021; Accepted 28 December 2021
Available online 29 December 2021

dose of 7-O-b-D-glucuronide (scutellarin) was reduced from 50 nM to 15 nM by ultrasound irradiation (1 MHz, 1 W/cm^2) in the treatment of human tongue cancer xenografts [17]. In another study, Bernard et al. demonstrated that US (0.5–1 W/cm^2) increased the effect of Cis on human ovarian cancer cells A2780/A2780cis [18]. However, almost half of the A2780cis ovarian cancer cell population in this study was suppressed at high cisplatin concentrations and 10-minute US therapy, relatively long treatment duration. For these reasons, this strategy is not efficient enough to overcome drug resistance. Thus, a lower concentration and shorter duration of treatment is essential for an effectively applicable strategy to defeat chemoresistance in cancer.

Owing to the advancement of nanomedicine, ultrasound agents are utilized to increase the efficiency of acoustic energy [15,19,20]. Gold nanocones (AuNCs), which are among the solid cavitation agents, are distinguishable for their efficient use of acoustic energy, simple synthesis, and biocompatibility [19,21]. Huang et al. have developed a therapeutic platform based on PEG-AuNCs, which they synthesized in liquid–liquid-gas three-phase for simultaneous photoacoustic (PA) imaging and photothermal therapy (PTT) applications [22]. They showed that PEG-AuNCs had good biocompatibility, ultra-high photothermal conversion efficiency ($\eta = 74\%$), simultaneous thermal and PA imaging, and PTT activity. In another study, Mannaris et al. showed that the same AuNCs are ultrasound-active, and the penetration of AuNCs is increased in the presence of ultrasound energy under in vitro conditions [23].

Here, we demonstrated the effect of nanoparticle-assisted and US therapy-mediated low-dose chemotherapy in terms of triple combination therapy to overcome the drug resistance problem on both 2D and 3D drug-resistant ovarian cancer cell models. Briefly, AuNCs were synthesized with the oil-in-water emulsion method and used to enhance the mechanical effect of US therapy. The cell membrane porosity, which was increased by the effect of US and AuNCs, was boosted the concentration of intracellular Cis accumulation and was effective in reversing Cis drug resistance at a low-dose drug concentration. With the triple combination therapy US + AuNCs + Cis, 60% of the drug-resistant cell population and approximately 83% of the colony formation were suppressed under the circumstance of the low-dose Cis. In addition, the efficacy of our developed triple combination therapy was shown in the A2780cis ovarian cancer 3D cell model with a 60% suppression of spheroid formation. Our results showed that triple combination therapy of the US + AuNCs + Cis was effective for drug-resistant ovarian cancer cells treatment and has high potential to reduce the side effects of chemotherapy by enabling therapy with low-dose drugs. Furthermore,this is the first study demonstrating the role of AuNCs, which increases the effectiveness of US, in overcoming drug resistance at the low-dose drug concentration.

2. Methods

2.1. Synthesis and characterization of AuNCs

AuNCs were synthesized according to a published protocol [21]. In brief, the contents of 0.8 mM gold (III) chloride hydrate ($HAuCl_4$; Sigma, USA) in 5 mL dH_2O were preheated to 45 °C for 5 min. 20 mM o-phenetidine (Sigma, USA) in hexane (Sigma, USA) solvent was prepared and slowly poured into preheated $HAuCl_4$ in dH_2O. The mixture was then placed into a sonicator (Alex Machine, India) and sonicated at 45 °C for 2 h to form cone-shaped AuNCs. With the oil-in-water emulsion method, the gold particles collected between two liquid phases induce the transformation of shape into in gold with the collapse of evaporated hexane bubbles. At the end of the sonication process, the mixture turned into opaque and purple color and was left to phase separation overnight. Thereafter, the supernatant was discarded, and the AuNCs was collected by centrifugation at 10,000 rpm for 20 min and washed with dH_2O three times, then re-suspended in dH_2O. The collected AuNCs were stored at 4 °C for further characterization. UV–vis absorption spectra were measured with a UV–vis spectrophotometer (Perkin Elmer Lambda 25, USA). The hydrodynamic diameter of AuNCs was determined by dynamic light scattering (DLS; Malvern Instruments, UK) using Zetasizer Nano ZS (Malvern Instruments, UK). The size and shape were shown by scanning transmission electron microscopy (STEM; Zeiss, Germany) after 10 µl of AuNCs were dropped onto a copper grid and air-dried. The concentration of AuNCs was determined with a Nanoparticle Tracking Analysis system (NTA, Malvern Instrument Nanosight NS300, UK).

2.2. Cell culture

In this study, two ovarian cancer cells A2780 (sensitive) and A2780cis (Cis-resistant) were used, which were kindly gifted by Prof. Hulya Ayar Kayali (Izmir Biomedicine and Genome Center, Izmir / Turkey). The cells were grown in complete RPMI-1640 (Biological Industries, Israel) medium supplemented with 10% fetal bovine serum (FBS; Biological Industries, Israel), 1% Pen-Strep (Biological Industries, Israel) at 37 °C, 95% humidity, and 5% CO_2 atmosphere. In order to maintain the resistance of A2780cis ovarian cancer cells, the cells were cultured with 1 µM Cis added medium.

2.3. Treatment of A2780/A2780cis cells

A 5 cm^2 therapeutic ultrasound probe (TUS; Roscoe, Soundcare Plus, Ohio/USA) was used for US treatments. Seven treatment groups were created as follows: untreated, Cis, AuNCs, US, US + Cis, US + AuNCs, and US + AuNCs + Cis. In our previous study, the effect of 1 MHz, 1.0 W/cm^2, 50% DC, 3 min acoustic wave on overcoming drug resistance of A2780cis by the treatment with the US and 11.7 µM cisplatin was shown. Our results demonstrated that a 1 MHz, 1.0 W/cm^2, 50% DC, 3 min acoustic wave has the ability to overcome drug resistance by suppressing 35% drug-resistant cell population compared to the Cis-only treatment group. Therefore, in this study, the similar acoustic wave was utilized to treat ovarian cancer cells. In addition, Cis (Kocak Farma, Turkey) at the IC_{50}concentration (4.3 µM) of the A2780 calculated in our previous study, which was approximately three times lower than the IC_{50} concentration of A2780cis cells. 40,000 of A2780 and A2780cis cells were separately seeded in 6-well plates. In AuNCs treatment groups, the number of AuNCs were measured with the NTA system and $4.6x10^8$ particles per mL (100 µg/mL) were added to each well and incubated at 37 °C for 2 h before the US treatment in accordance with the previous study in the literature [22]. 4.3 µM Cis was added and the US was applied immediately after the drug was added. Following 6 h of incubation at 37 °C, US therapy was repeated, and the cells were left incubated for a further 42 h, which corresponded to a total treatment time of 48 h. The resazurin and calcein-based cell viabilities were performed after a total of 48 h of incubation time.

2.4. Cell viability

Cell viability experiments with resazurin were performed according to the published study to illustrate the change in metabolic activity in living cells after the treatment [24,25], and Fig. 1 shows the design of the experiment. Briefly, 40,000 A2780 or A2780cis cells/well in the medium were seeded in the 6-well plates. Treatment groups were defined as untreated, AuNCs, Cis, US (1 MHz, 1.0 W/cm^2, 50% DC, 3 min), US + Cis, US + AuNCs, and US + AuNCs + Cis, and the cells were treated as described. After 48 h of total incubation at 37 °C, the medium was replaced by 1x resazurin, and then the viability of the cells was determined after 3 h incubation with a fluorescent microplate reader (Promega Glomax-Multi, WI, USA) using with a green filter (510–560 nm). The viability of the cells was calculated from the fluorescence intensities of each value by normalized with the untreated group.

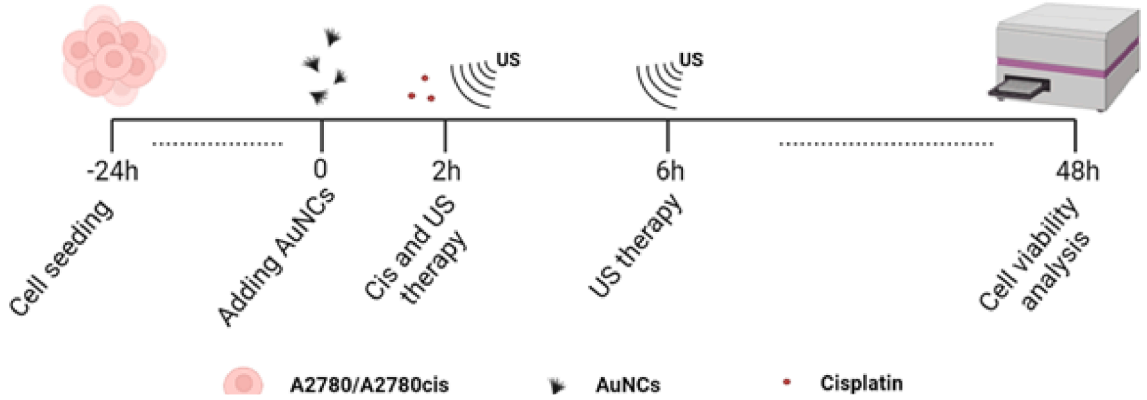

Fig. 1. Timeline of the study. 40,000 A2780/A2780cis cells were separately seeded in each well. 2 h after the addition of 100 μg/mL AuNCs;4.3 μM of Cis and US therapy were applied. After 6 h, US therapy was applied again, and after 48 h of incubation, cell viability analyzes were performed.

2.5. Visualizingthe effect of triple-combination treatment on A2780 and A2780cis cells

To visually compare the effects of untreated, and Cis, AuNCs, US, US + Cis, US + AuNCs, and US + AuNCs + Cis treatments in A2780/A2780cis ovarian cancer cells, calcein-based cell viability assay, which interacts with living cells to emit green fluorescence, was performed according to the previously published protocol [27]. The treatments were carried out as previously described. After 48 h, RPMI-1640 medium was replaced with 3 μM of calcein (green) (Thermo Fisher Scientific, USA) which was dissolved in dimethyl sulfoxide (DMSO, Sigma, USA) and diluted with RPMI-1640. The cells were incubated for 2 h and the dye solution was carefully replaced with the culture medium. The images were captured using an inverted fluorescent microscope (Leica, DMI8 Automated, Germany). The green fluorescence intensities of the images were calculated with ImageJ.

2.6. Cell cycle analysis

The cell cycle analysis was also performed as previously reported study [26] in A2780 and A2780cis ovarian cancer cell lines using propidium iodide (PI;Sigma, ≥94.0% (HPLC), USA) staining to identify the potential arrest resulting from treatment with Cis-only, US, US + Cis, US + AuNCs, and US + AuNCs + Cis. Briefly, cells were seeded in a 6-well plate (100,000 cells each plate). Before the treatment, the cells were synchronized for 2 h in a FBS-free medium. Treatment groups including AuNCs were treated with the US, 2 h after the addition of 100 μg/mL AuNCs; and treatment groups including Cis were treated with the US, immediately after the addition of 4.3 μM Cis. US therapies were applied twice in total with a 6 h interval. 21 h after the treatment the cells were collected, washed with PBS and resuspended in 70% ice-cold EtOH (Merck, Germany), and incubated overnight at −20 °C. The cells were collected again and washed twice with PBS and treated with 200 μl of 50 mg/mL RNase (Thermo Fisher Scientific, USA) for 30 min at 37 °C, then stained with PI. Cell cycle analysis was performed by flow cytometry (BD FACSAriaTM III, New Jersey,USA), using the FL2-A channel. 10,000 events were evaluated for each sample. The collected data were analyzed with FlowJo 10.8 software. The results were presented as the percentages of G1, G2/M, S, and sub-G1 (apoptotic) phases.

2.7. Determination of intracellular Cis and AuNCs concentrations

Inductively coupled plasma mass spectroscopy (ICP-MS; Agilent 7500A, California, USA) technique was carried out according to the previous study [27] to evaluate the effect of treatment on the concentration of intracellular platinum and gold ions. 40,000 A2780cis cells were seeded into six-well plates and incubated for 24 h for attachment. After the treatment, the cells were detached and lysed using 200 mL of lysis buffer (Pierce RIPA Buffer, Thermo Fisher Scientific, USA). The lysed cells were digested by adding 0.5 mL of freshly prepared aqua regia (highly corrosive) and incubated for 15 min. Then each sample volume was completed to 10 mL with dH_2O and analyzed for Cis and AuNCs content. Each sample was measured three times.

2.8. Colony formation assay

A colony formation assay was performed to determine the effect of untreated, Cis, US, US + Cis, US + AuNCs, and US + AuNCs + Cis treatments on the long-term ability of cells to survive and proliferate to form colonies. 100 μg/mL AuNCs were added 6-well plate containing 100,000 number of A2780/A24780cis cells in each well. US treatment was applied after adding Cis to the Cis treatment groups. 2 h after the first US treatment, cells were harvested with trypsin and re-seeded in 12 well-plates at 300 cells per well. After 10 days, the medium was discarded, and the cells were stained with 1.0 % crystal violet (Sigma, USA) in 10.0 % methanol. After 10 min incubation at RT, the mixture was discarded from the wells. The wells were washed with PBS to clean up excess crystal violet. Colonies containing 50 or more cells were counted as one colony.

2.9. Determination of the effect of triple-combination treatment on A2780 and A2780cis 3D spheroid models

3D spheroid was designed to compare the effects of untreated, and Cis, US + Cis, US + AuNCs + Cis treatment groups in the 3D cell model. A2780 and A2780cis spheroids were prepared according to our published protocol [15]. Shortly, 5.0% (w/w) of polyethylene glycol (PEG, 35 000 Da, Sigma) and 12.8% (w/w) of dextran (500,000 Da, Sigma) solutions were prepared in the culture medium. The surface of each well of the 6-well plate was covered with 1 mL of a 2% agarose solution (w/v) to obtain a non-adherent surface. After the agarose solution was cooled down, all wells were washed with PBS, and then 1 mL of 5.0% (w/w) PEG solution was added to each well. A2780 and A2780cis cells were collected, and 1,000,000 cells were suspended in 3 μl of 12.8% (w/w) aqueous dextran. The cell suspension was added to each well. Because of the immiscible property of PEG and dextran, cells aggregated at the interface at 24 h to occur the spheroid form. Then, 100 μg/mL of AuNCs was added to the treatment groups containing AuNCs, and 2 h later,4.3 μM Cis was added to the cis treatment groups followed by US therapy immediately. After 48 h, the viable spheroids were assayed with the calcein dye as previously described, and fluorescence microscopy images were captured to calculate green fluorescence intensity of viable

spheroids by using ImageJ.

2.10. Statistical analysis

Statistical testing used one-way analyses of variance (ANOVA) for multiple comparisons. All statistical analyzes were performed with GraphPad Prism 8.0 and all tests with *p values of* < 0.05 were indicates statistically significant difference between groups..

3. Results and discussion

3.1. Characterization of AuNCs

AuNCs were used to increase of the effectiveness of US therapy in A2780/A2780 cells and tumor spheroid models. The data confirmed the successful synthesis of AuNCs as demonstrated in previous studies in the literature [23]. According to STEM images (Fig. 2**a, b)**, AuNCs have a cone-shaped structure that opens outwards and attracts attention with their rough structure in their large surface area. According to the DLS results (Fig. 2**c)**, the size of the particles were around 100 nm, which was confirmed by the STEM images. According to the results of ZetaSizer (Fig. 2**d)**, the particles had positive charges, unlike the common citrate reduced gold nanoparticles in the literature [28]. Studies in the literature have emphasized that there is a strong correlation between the amount of positive charge of nanoparticles and their internalization into cells [29]. This is due to the electrostatic interaction between the negatively charged cell membrane and the positively charged particles. Therefore, another hallmark trait of AuNCs is that they are positively charged. The concentration of AuNCs was determined as $3.6x10^{11}$ particles mL^{-1} according to the result obtained from the NTA measurements (Fig. 2**e)**.

3.2. With US + AuNCs + Cis the amount of intracellular Cis and AuNCs increases, drug resistance decreases, and more cell deaths are triggered

Resazurin and calcein-based cell viability assays were performed to compare the effectiveness of the various therapies on Cis resistance. The effects of treatment groups on the change on cell population were visually demonstrated by staining with calcein. ICP-MS analysis was performed to show the effect of US + AuNCs + Cis combination therapy on intracellular Cis and AuNCs accumulation in A2780cis ovarian cancer cells.

According to the results of the A2780 resazurin-based cell viability assay performed according to the experimental setup in Fig. 1, the viability was 92.5% in AuNCs, 55.7% in Cis-only, 67.4% in US 63.5% in US + AuNCs, 22.1% in US + Cis, and 11.7% in US + AuNCs + Cis triple combination therapy compared to the untreated group (Fig. 3**a)**. In A2780 ovarian cancer cells, the triple combination therapy resulted in a significant decrease in cell viability. Exposure to US disrupted cell membrane integrity, reduced cell viability [30], and we found that approximately 33% of A2780 ovarian cancer cells in the US treatment group were suppressed compared to the control group. The effect of cisplatin on A2780 cells was increased by US therapy: there was 33.6% more cells death with the US + Cis therapy compared to the Cis treatment group. Moreover, AuNCs increased the effectiveness of the US therapy, which together triggered greater cell suppression by increasing the effectiveness of Cis. While there was no statistically significant difference between US and US + AuNCs treatment groups, more cell death occurred with the addition of Cis to the US + AuNCs + Cis combination therapy. Based on the results of the A2780 calcein cell viability assay, viability was 44.1% for Cis, 50.0% for the US, 53.1% for US + AuNCs, 24.8% for US + Cis, and 7.5% for US + AuNCs + Cis combination therapy compared to the untreated group(Fig. 4**a, b)**. The calcein viability results support the resazurin-based viability results of A2780 ovarian cancer cells. The effectiveness of Cis was increased by the US treatment: 19.3% more cells were suppressed in the US + Cis treatment group compared to the Cis-only treatment group. On the other hand, the effectiveness of Cis was increased by US + AuNCs in the triple combination therapy, a significant decrease in the cell population compared to the other treatment groups occurred: 36.6% more cells were treated with the combined treatment than with the Cis-only treatment group alone.

The effects of treatment groups to reserve drug resistance with lower drug concentration on A2780cis ovarian cancer cells were compared between resazurin and calcein viability assays. The results showed that the triple combination therapy US + AuNCs + Cis was successful in combating the resistance of A2780cis cells with low-dose chemotherapy (treatment with Cis at the IC50 value of A2780 cells). According to the

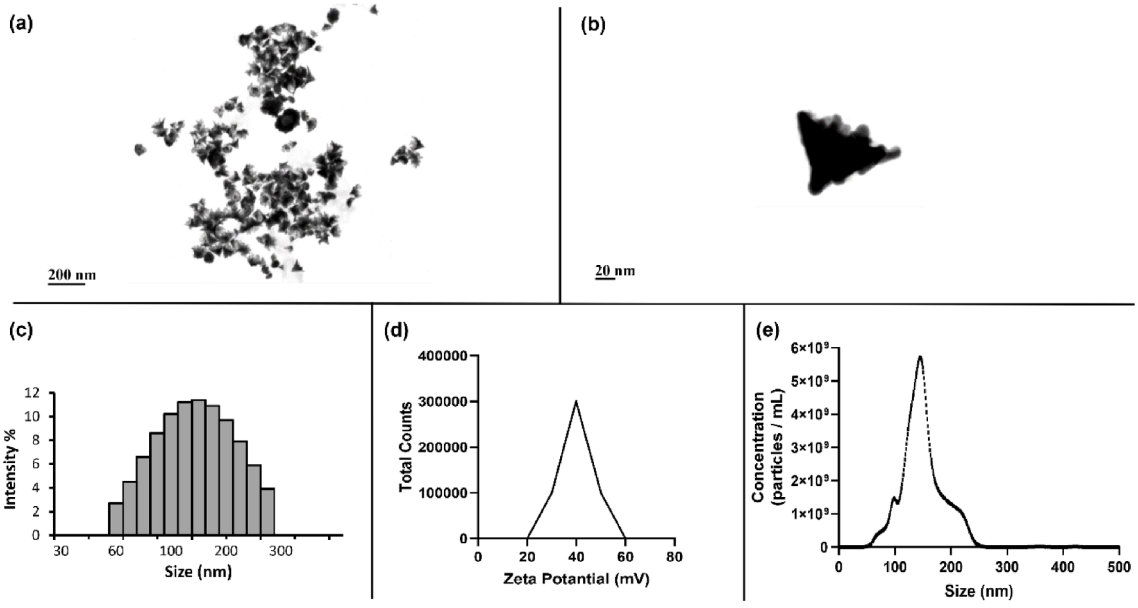

Fig. 2. Characterizations of AuNCs. Images captured by STEM (scale bar 200 and 20 nm) **(a,b)**, size distribution of AuNP measured by DLS **(c)**, particle charge measurement obtained with ZetaSizer **(d)**, and size vs concentrations of AuNCs analyzed with NTA **(e)**.

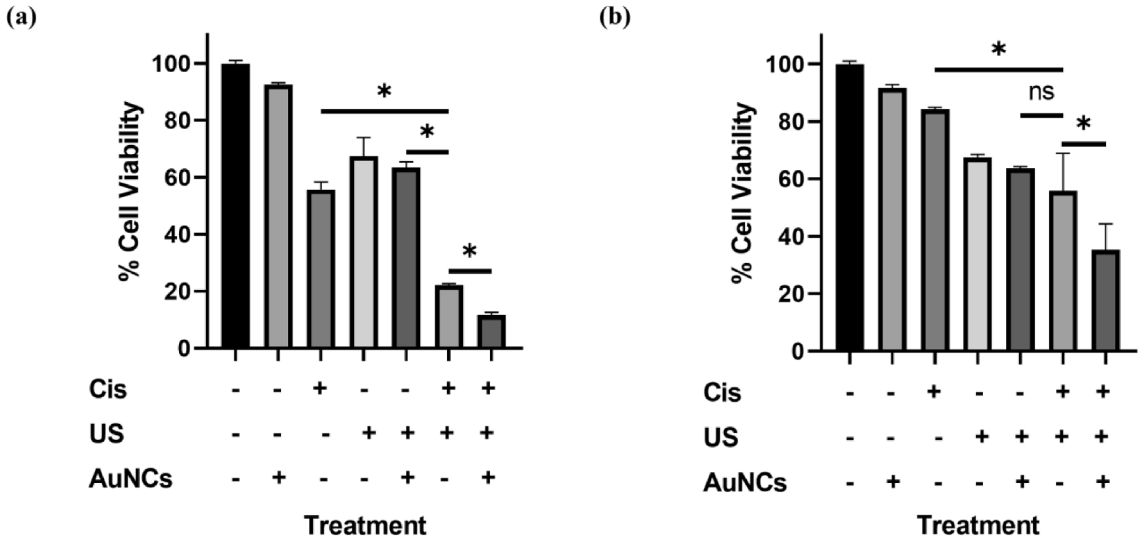

Fig. 3. Effect of Cis, US, US + AuNCs, US + Cis, and US + AuNCs + Cis treatments on cell viability in A2780/A2780cis ovarian cancer cell lines. A2780 **(a)** and A2780cis **(b)** ovarian cancer cells were treated separately with Cis, US, US + AuNCs, US + Cis, and US + AuNCs + Cis combination therapy, and cell viability was analyzed with resazurin 2 days after treatments. (*p-values < 0.05).

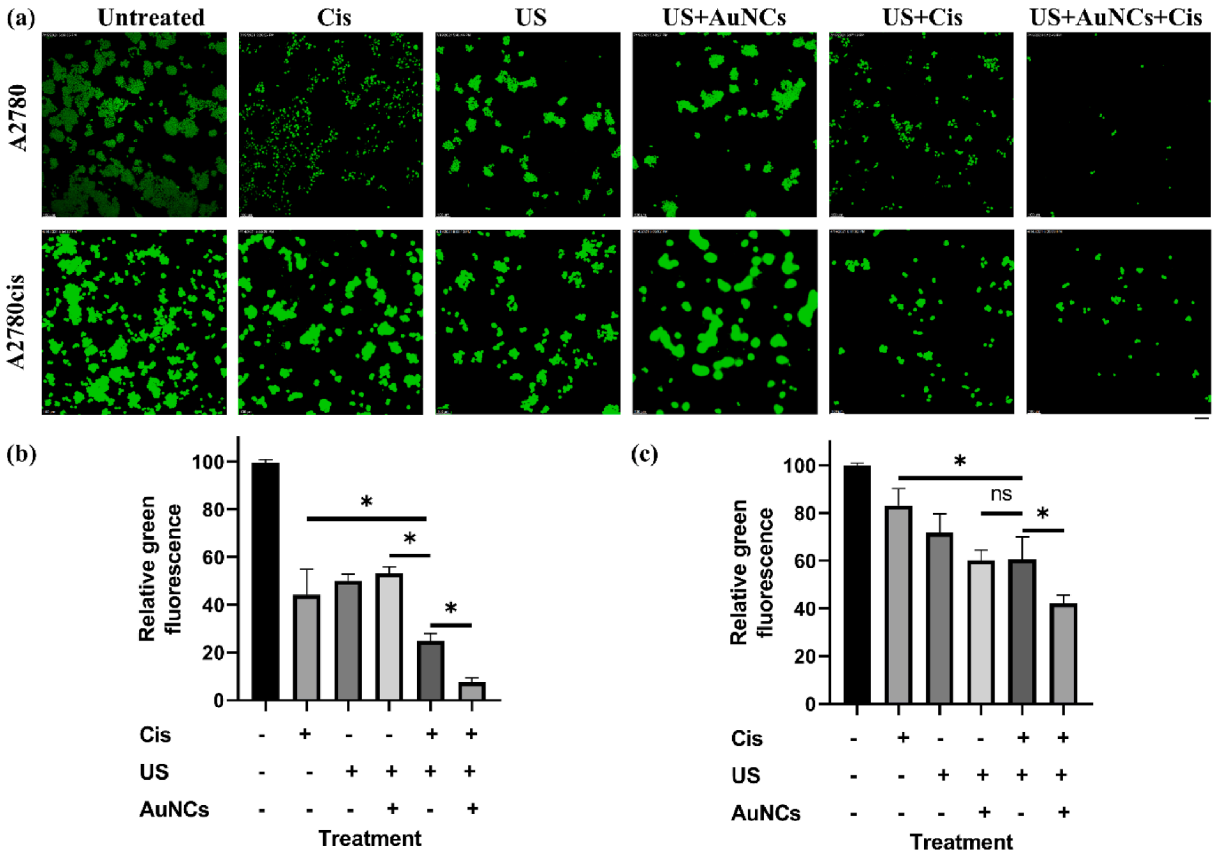

Fig. 4. Fluorescent images of calcein stained A2780/A2780cis cells. The cells were incubated at 37 °C and stained with calcein, where live cells appear as green fluorescence **(a)**. Quantitative analysis of fluorescence from calcein-positive cells (green) for A2780 **(b)** andA2780cis **(c)**. Green fluorescence intensity was calculated by using ImageJ. All images have been taken at 100 × magnification; the scale bar is equal to 100 μm. The field of vision was randomly selected for all the samples. (*p-values < 0.05).

results of the A2780cis resazurin-based cell viability assay, viability was 91.6% for AuNCs, 84.2% for Cis-only, 67.4% for the US, 63.7% for US + AuNCs, 55.8% for US + Cis, and 35.3% in the triple combination therapy US + AuNCs + Cis when compared to the untreated group (Fig. 3**b**). US therapy also increased the sensitivity to Cis on drug-resistant cells: there was 28.2% more cell death with the US + Cis treatment compared to the

Cis treatment group. AuNCs increased the effectiveness of the US therapy so that the therapeutic effect of Cis was boosted on A2780cis compared to the effect chemotherapy (Cis-only). Whereas the combined US + AuNCs + Cis treatment with the low-dose drug was almost two times more successful in killing the A2780cis cell population than the only Cis drug. Based on the results of the A2780cis calcein cell viability assay, viability was 44.1% for Cis-only, 50% for the US, 53.1% for US + AuNCs, 24.8% for US + Cis, and 7.5% for US + AuNCs + Cis combination therapy when compared to the untreated group (Fig. 4**a, c**). The effectiveness of Cis was raised by the US treatment: 22.5% more cells were suppressed in the US + Cis treatment group compared to the Cis-only treatment group. On the other hand, the effect of Cis was increased by US + AuNCs in the US + AuNCs + Cis combination treatment group, a significant decrease in viability was monitored in the cell population at US + AuNCs + Cis compared to the other treatment groups: 41% more inhibition of cell viability was provided with the combined treatment compared to the Cis-only treatment group. The results obtained from both resazurin and calcein viability assay results confirmed each other.

According to the results of ICP-MS analysis on A2780cis ovarian cancer cells, platinum ion accumulation of 0.081 ppb/protein (μg/mL) was observed in the US + Cis treatment group and 0.114 ppb/protein (μg/mL) in the US + AuNCs + Cis treatment group (Fig. 5**a**), while 16.918 ppb/protein (μg/mL) in the US + AuNCs treatment group and 36,059 ppb/protein (μg/mL) in US + AuNCs + Cis treatment group (Fig. 5**b**) gold ion accumulation was observed. These results support that the triple combination therapy increases the intracellular accumulation of Cis and AuNCs in the drug-resistant cell line. With the combined therapy, 1.4 times more intracellular Cis accumulation was observed compared to the US + Cis treatment group. These results show that AuNCs increase the effect of the US and that more Cis is taken up by increasing the membrane porosity. Moreover, the accumulation of intracellular AuNCs with combination therapy was 2.1 times higher than with US + AuNCs. The accumulation of intracellular AuNCs occurs more strongly in the presence of Cis which indicates the synergistic effect of AuNC and Cis [31].

According to these results, the US + AuNCs + Cis combination therapy demonstrated effectiveness with its enhanced treatment compared to the other treatment groups. Due to the fact that the contribution of the mechanical effect of the US was elevated in the presence of AuNCs, the intracellular Cis concentration was increased. Thus, the triple combination therapy exhibited superior therapeutic activity with a higher number of Cis inside the cisplatin-resistant cells. A2780cis drug-resistant cells were also successfully treated with the Cis IC_{50} concentration of the A2780, Cis-sensitive cells. In triple combination therapy, about 90% of the cell population was suppressed in A2780 cells, while almost 60% of A2780cis cells were suppressed at the same dose of Cis. In addition, in reduction in the side effects of chemotherapeutics through the use of low-dose active drug concentration is another advantage of our triple combination therapy. Furthermore, in the literature, in order to overcome the drug resistance in A2780cis ovarian cancer cells, the cells were treated with IC_{50} of Cis and then ultrasound waves in the form of a continuous-wave of 1 MHz, 10 min applied [18]. The concentration of the drug used against A2780cis in the reference study was relatively higher than our study and could therefore not reduce the non-specific toxicity of chemotherapy. In addition, the duration of the treatment was relatively long. On the other hand, our triple combination therapy showed a successful effect in treating drug-resistant ovarian cancer cells with the low-dose drug and a short treatment duration, and US + AuNCs + Cis triple combination therapy caused more cell suppression compared to that study. In addition, AuNCs play a prominent role in triple combination therapy both in creating a synergistic effect with cisplatin and in increasing the effectiveness of US.

3.3. *US + AuNCs + Cis triple combination therapy reduces colony formation*

The colony formation assay was performed to demonstrate the long-term therapeutic effect of US + AuNCs + Cis triple combination therapy

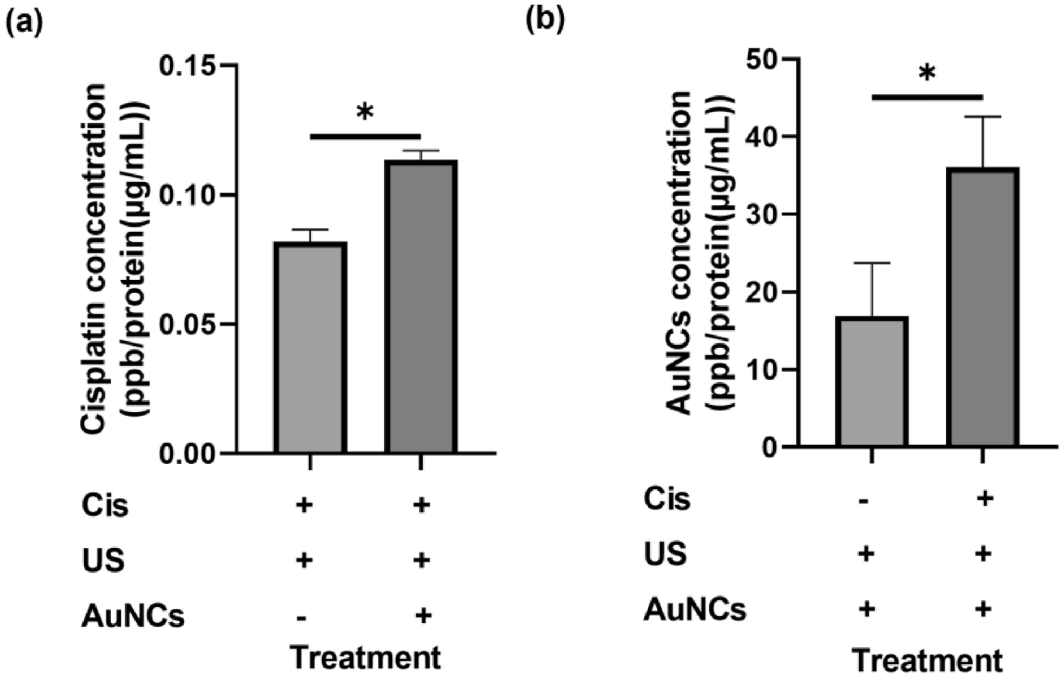

Fig. 5. Intracellular Pt and Au concentrations. Pt concentrations in A2780cis ovarian cancer cells after treatment with US + Cis and US + AuNCs + Cis combination therapy **(a)**, and Au concentrations in A2780cis ovarian cancer cells after treatment with US + AuNCs and US + AuNCs + Cis combination therapy **(b)**. Intracellular concentrations of Cis and AuNCs were measured in ppb Pt/Au per protein concentration (μg/mL). (*p-values < 0.05).

in A2780 and A2780cis ovarian cancer cells. Colony formation is one of the main methods in drug discovery and it shows the ability of individual cells to form tumor colonies [32] and long-term efficiency of treatment [33].

According to the results in A2780 ovarian cancer cells, colony formation was 15.2% for only Cis, 60.5% for the US, 44.8% for US + AuNCs, 11.1% for US + Cis, 2.8% for US + AuNCs + Cis combination therapy compared to the untreated control group (Fig. 6**a, b**). In the triple combination therapy, more effective results were obtained in the long-term treatment strategy compared to the other treatment groups: Clonogenic viability was decreased about 97% in US + AuNCs + Cis treatment. Interestingly, in contrast to the cell viability experiments, a statistically significant difference was observed between the US and US + AuNCs treatment groups. This might be because of the ability of gold nanoparticles to inhibit colony formation [34]. In addition, it was observed that the addition of AuNCs in the US + Cis therapy reduced the resistance developed against Cis under the US therapy: 8.3% less colony formation was observed in the US + AuNCs + Cis triple combination therapy compared to the US + Cis treatment group.

According to the results obtained from A2780cis treatments, colony formation was 42.4% with Cis-only, 75.5% with the US, 55.6% with US + AuNCs, 29.8% with US + Cis, 17.4% with US + AuNCs + Cis therapy compared to the control group (Fig. 6**a, c**). The triple combination therapy US + AuNCs + Cis was successful in suppressing the colony forming abilities of each individual cell, and our results showed that the triple combination therapy had a long-term therapeutic effect on resistant cells with low dose drug concentration, almost 83% of colony formation was suppressed. In addition, a statistically significant difference was observed between the US and US + AuNCs treatment groups in A2780cis cells.

In summary, in the context of the long-term therapeutic efficacy of the treatments, the colony formation test showed that colony formation in the US + AuNCs + Cis combination therapy was successfully suppressed in both cell lines. In A2780cis cells in particular, the therapeutic effect of the triple combination therapy with low-dose Cis concentrations is promising in order to reduce the side effects of chemotherapy. In addition, AuNCs potentiated the effects of US on both cell lines and played an important role in suppressing colony formation.

3.4. Triple combination therapy affects cell cycle arrests of ovarian cancer cells

Cells with DNA damage are arrested during their cell cycle and these arrests lead the cells to apoptosis [35]. Cancer cells, especially drug-resistant cells; however, usually overcome the cell cycle arrest and can continue their cycle with damaged DNA [36]. Cis is a type of chemotherapeutic agent that penetrates the cell nucleus and induces DNA breaks to direct cells apoptosis [37]. With their efflux mechanism, *cis*-resistant cancer cells can reduce the intracellular drug concentration and escape DNA damage caused by Cis [38]. Here we used US + AuNCs + Cis to increase the internalized concentration of Cis with the effect of an increased US activity of AuNCs. To confirm the apoptotic activity of Cis, the difference in cell cycle phase distributions of the sensitive and resistant cells between untreated and treatment groups was determined.

The results in A2780 cells were as following: Untreated (Sub-G1 2.0%, G1 56.2%, S 22.7%, G2/M 18.5%), Cis (Sub-G1 0.4%, G1 3.6%, S 19.5%, G2/M 76%), US (Sub- G1 60.4%, G1 19.7%, S 8.1%, G2/M 11.4%), US + Cis (Sub-G1 74.2%, G1 13.5%, S 8.5%, G2/M 3.5%), US +

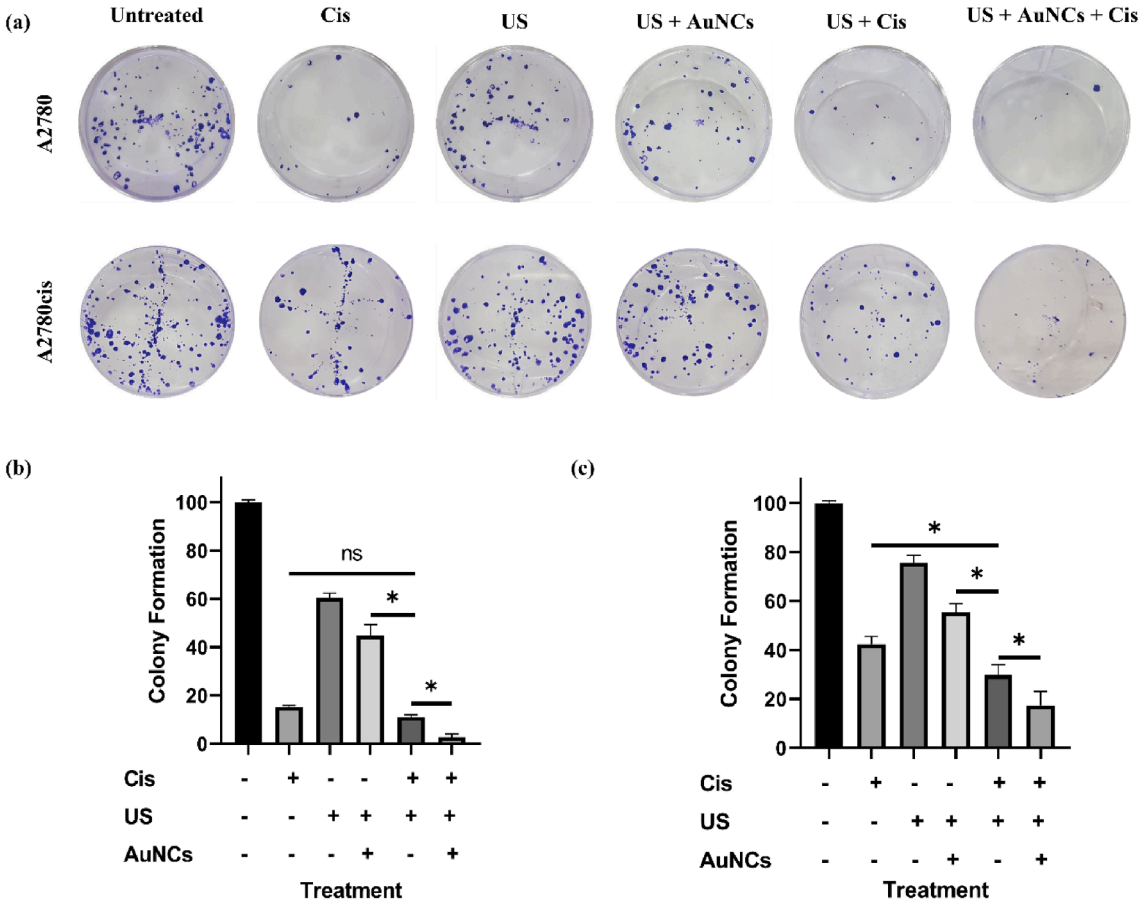

Fig. 6. Colony formation assay using A2780/A2780cis was performed as described in the experimental procedure **(a)**. Bar graph of colony formation assay results of A2780 **(b)** andA2780cis **(c)** by counting the number of colonies containing over 50 cells. (**p-values < 0.05)*.

AuNCs (Sub-G1 63.8%, G1 19.0%, S 12.4%, G2/M 4.9%), US + AuNCs + Cis (Sub-G1 93.8%, G1 3.9%, S 2.1%, G2/M 0.1%) (Fig. 7**a**). For A2780 ovarian cancer cells, the ability of US therapy to most severely stop cells in Sub-G1 was observed in 60.4% of the cell population. Adding Cis to US therapy resulted in more cells being arrested in sub-G1 (13.8% more cells with US + Cis therapy compared to US therapy). Interestingly, there was no statistical difference between US and US + AuNCs therapies, that is, AuNCs did not change the effects of US on the cell cycle stage, whereas almost the entire cell population (93.8%) accumulated in Sub-G1 in the US + AuNCs + Cis combination therapy. This might be related to US + AuNCs therapy increasing the effectiveness of Cis. While more cells accumulated in Sub-G1 in the US + Cis treatment compared to the US group, more cells were arrested in Sub-G1 in the Cis therapy, the effectiveness of which was increased by US + AuNCs.

In A2780cis, there was no significant change in Sub-G1 in all groups. Nevertheless, significant changes in the G1 and S phases were found in treatments containing Cis. The results in A2780cis cells were as following: Untreated (Sub-G1 2.0%, G1 57.5%, S 17.8%, G2/M 21.8%), Cis (Sub-G1 0.5%, G1 27.9%, S 44.9%, G2/M 25.1%), US (Sub- G1 2%, G1 48.7%, S 23.1%, G2/M 25.8%), US + Cis (Sub-G1 0.6%, G1 29.0%, S 42.7%, G2/M 26.0%), US + AuNCs (Sub-G1 8.7%, G1 44.9%, S 21.5%, G2/M 24.0%), US + AuNCs + Cis (Sub-G1 3.3%, G1 35.8%, S 34.7%, G2/M 25.0%) (Fig. 7**b**). The cell cycle analysis was different for cis resistant A2780cis cells treated with low-dose Cis. It was observed that more cells accumulated in the S and G2/M stages with US therapy compared to the control group. When the US + Cis group is compared with the US + AuNCs + Cis therapy, the effect of AuNCs in the triple combination therapy to shift more cells to the G1 and sub-G1 stage: Compared to the US + Cis treatment group, 6.8% more cells accumulated in the G1 and 2.7% more cells in the sub-G1 stage in the triple combination therapy. Compared to the control group, more cells were arrested at the S stage in the US + AuNCs + Cis triple combination therapy. In addition, when comparing the results of Cis and triple combination therapy, 44% of the cells accumulated in the S phase in the Cis-only treatment group, whereas, in the triple combination therapy, the percentage of arrested cell population in the S phase decreased and accumulated more in the G1 and Sub-G1 phases. According to our results, while most of the cells accumulated in G1 under the influence of US therapy in A2780cis cells, and there was a significant increase in sub-G1 under the impact of US + AuNCs therapy with the increase of mechanical effect compared to US therapy. According to these results, in the triple combination therapy compared to the Cis treatment group, cells accumulated more in the Sub-G1 and G1 phases, both with the effect of US and with the effect of US + AuNCs, compared to the Cis-only treatment group.

The sub-G1 population indicated an increase in apoptotic cells under US therapy. In particular, the sensitive cells more affected by the US than drug-resistant ones. In A2780 cells, there was no significant Sub-G1 in the untreated and Cis groups, while the percentage of Sub-G1 population was approximately 94 in triple combination treatment (Fig. 7**a**). However, only the US treatment showed at least 60% Sub-G1, which indicated greater disruption of the membrane integrity by the US. This is likely because A2780 cells were more susceptible and sensitive to stressful conditions than A2780cis cells according to the results demonstrated in our previous study (data not shown). Our previous study examined the effect of US therapy on both A2780 and A2780cis ovarian cancer cells. 46.7% of the A2780cis ovarian cancer cell population were arrested in G1 phase while 58.9% of the A2780 cell population were arrested in Sub-G1. This is most likely because of the difference in stiffness of cell membrane of A2780 and A2780cis since Sharma et al. showed that the membrane of cisplatin-resistant ovarian cancer cells is stiffer than the form of drug-sensitive cancer cells [39]. Therefore, A2780cis cells may show resistance against the mechanical effect of US therapy. Similarly, in this study, A2780cis cells accumulated mostly in the G1 phase under the mechanical effect of US therapy. In US + AuNCs therapy, more cells accumulated in the Sub-G1 phase compared to US therapy. This is because, in A2780cis cells that were resistant to US therapy, more cells were arrested in Sub-G1 with the increased mechanical effect with US + AuNCs. These results confirm the hypothesis that AuNCs increase the efficacy of US therapy. Treatment with US + AuNCs + Cis ultimately caused the highest apoptotic population among all treatments.

In conclusion, the US has the ability to arrest the A2780 cells at the sub-G1 stage but not the A2780cis. The possible reason lies in the different cell structure of A2780 and A2780cis cell structure, as such cisplatin-resistant ovarian cancer cells are stiffer [39] which was shown in our previous study (data not shown). Moreover, it was observed that more cells were arrested in Sub-G1 in both cell lines with triple combination therapy.

3.5. *Triple combination therapy with the low-dose Cis suppresses drug-resistant ovarian cancer spheroids*

So far, the therapeutic effectiveness of the triple combination therapy US + AuNCs + Cis has been shown, which successfully treat drug-resistant cells in 2D cell cultures. However, more accurate mimicking of the tumor microenvironment model is a prerequisite for studying the effects of triple combination therapy. For this purpose, our developed strategy was examined in a 3D tumor cell model [40].

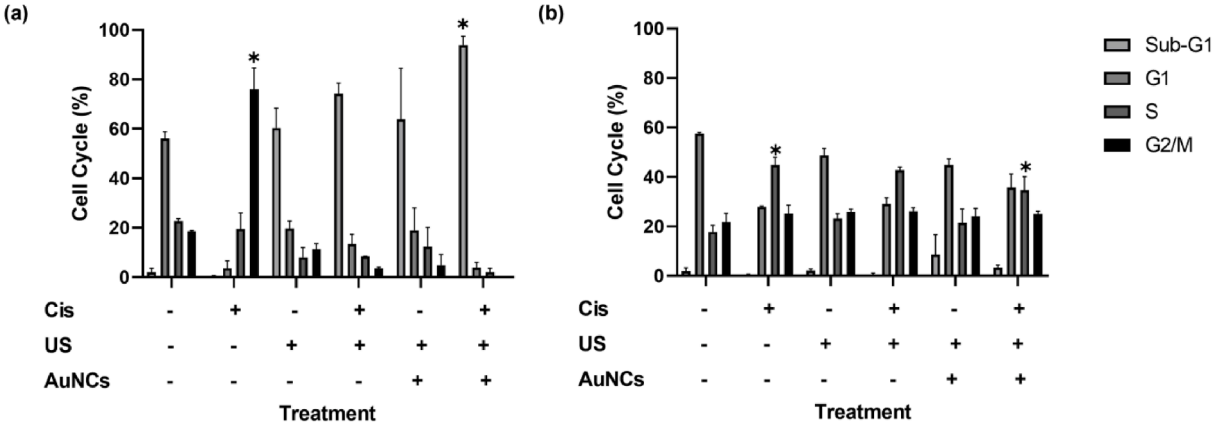

Fig. 7. Effect of treatment groups on cell cycle in A2780 **(a)** and A2780cis **(b)** cells. Cell cycle analysis was performed with the PI staining assay. A2780/A2780cis cells were stained with PI 21 h after Cis, US, US + AuNCs, US + Cis, and US + AuNCs + Cis treatments. Cell cycle analysis was performed using flow cytometry. (*p-values < 0.05).

2D cell culture model is frequently preferred because of its ease of use for the in vitro therapeutic activities [41,42]. However, 2D cell culture cancer models are far from the characteristics of in vivo solid tumor environment, and it has been shown that treatments that are effective in 2D cell cultures do not guarantee the same success in vivo [43]. The therapeutic effect of US + AuNCs + Cis triple combination therapy on drug-resistant cells with low-dose Cis was demonstrated in 3D cell models of drug-resistant ovarian cancer that well represented in vivo tumor characteristics and an idea of the effectiveness of treatment in the clinical stage [44].

According to the results in A2780 ovarian cancer cells, the proportion of viable spheroids was determined as 58.8% in Cis-only, 32.9% in US + Cis, and 22.4% in US + AuNCs + Cis combination therapy compared to the control group (Fig. 8**a, b**). It was statistically shown that the US treatment, which showed a sensitizing effect against Cis resistance in 2D cell culture, had the same effect in the 3D cell model: 25.9% more spheroids were treated by the US + Cis treatment group compared to Cis-only. In addition, a statistically significant decrease in 3D tumor model size was observed in the combination treatment group compared to the other treatment groups: 78% of the spheroid was treated compared to the control group. AuNCs increased the effectiveness of US therapy, allowing more spheroids to be treated in the triple combination therapy. There was a statistically significant decrease in the viability at US + AuNCs + Cis triple combination therapy compared to the US + Cis group, at 10.5% more spheroids were inhibited.

Results in ovarian cancer model A2780cis, the proportions of viable spheroid were determined in comparison to the control group as 89.1% in Cis-only, 53.6% in US + Cis and 40.2% in US + AuNCs + Cis (Fig. 8**a, c**). It was demonstrated that the treatment groups that showed treatment efficacy in 2D cell culture medium with low-dose Cis also showed the similar effect in the A2780cis 3D cell model. There was no treatment effect of low-dose Cis was observed in A2780cis cells, while sensitivity to Cis was increased under the US therapy, and 35.5% more spheroids were inhibited in the US + Cis treatment group. The combination therapy ensured effective therapeutic effect on the 3D cell model: Almost 60% spheroid suppression compared to the control group. In addition, AuNCs have played a role in reducing the resistance of Cis in a 3D cancer model with US therapy, 13.4% more spheroids were suppressed compared to the US + Cis treatment group.

Overall, it has been shown that the effectiveness of individual therapy is limited in both A2780 and A2780cis spheroid cell models. Low-dose Cis has limited success in treating drug-resistant cells, and higher concentrations of drugs are required to treat A2780cis cells. On the other hand, US therapy was successful in sensitizing spheroids to Cis in both

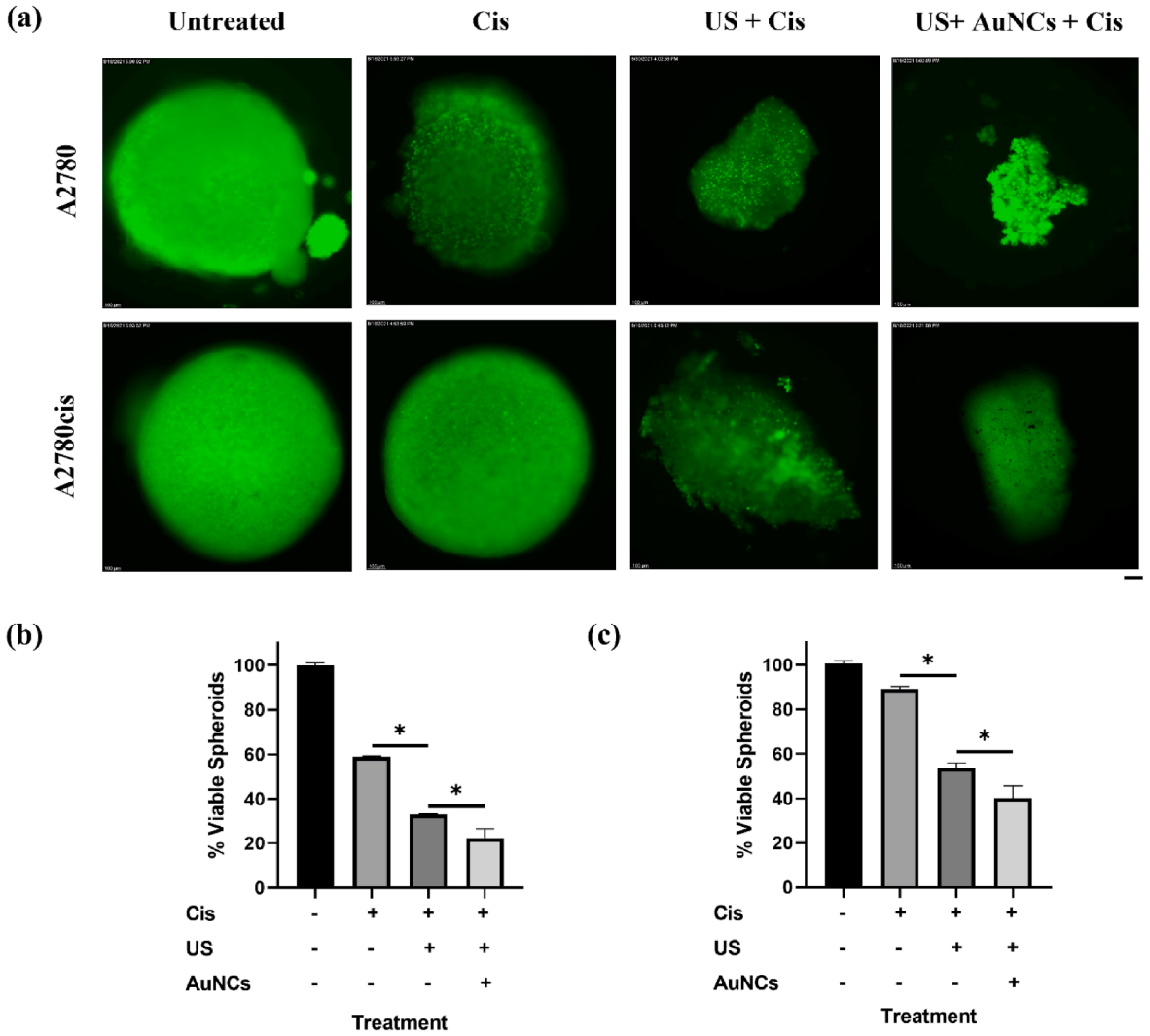

Fig. 8. The effect of Cis, US + Cis, and US + AuNCs + Cis combination therapy on A2780/A2780cis ovarian cancer spheroids. Fluorescent images of calcein stained A2780/A2780cis spheroids**(a)**. Quantitative analysis of fluorescence from calcein-positive spheroids (green) for A2780**(b)** and A2780cis**(c)**. Green fluorescence intensity was calculated by using ImageJ. All images have been taken at 100 × magnification; the scale bar is equal to 100 μm. (*p-values < 0.05).

cell models. Due to the high positive pressure of the solid tumor environment, it becomes difficult for the drug to reach the inside of the tumor and to exert its therapeutic effect [45–47]. Studies have shown that the US reduces the positive pressure within the tumor and increases the effectiveness of the drug by reaching the inner parts of the chemotherapy [48,49]. The efficacy of US therapy in spheroid models is promising that it might also show successful therapeutic efficacy in overcoming drug resistance in vivo solid tumor models. Moreover, it was also shown in both A2780/A2780cis spheroid models that AuNCs increased the efficiency of the US. US + AuNCs + Cis triple combination therapy ensured cancer treatment with low-dose Cis, especially in the A2780cis spheroid model. Our results showed that US + AuNCs + Cis triple combination therapy might also be an effective cancer therapy method in vivo and in clinical stages.

4. Conclusion

In this study, the effects of US + AuNCs + Cis triple combination therapy on drug-resistant ovarian cancer cells were investigated. The results show that our triple combination therapy with low-dose Cis effectively treats drug-resistant A2780cis ovarian cells. In addition, intracellular Cis accumulation was increased by the US, whose effect was enhanced by AuNCs, and triple combination therapy enabled the treatment of more cancer cell populations on both 2D and 3D A2780/A2780cis ovarian cancer models. Due to the triple combination therapy, US + AuNCs + Cis, approximately 60% of A2780cis cells and 83% of colony formation were suppressed. Furthermore, in the US + AuNCs + Cis triple combination therapy, AuNCs caused more cells to accumulate in sub-G1. These results show that triple combination therapy offers effective results in the long term. Our spheroid 3D cell model results demonstrated that US + AuNCs + Cis triple combination therapy could provide effective cancer treatment in vivo and in clinical stages. All in all, the US + AuNCs + Cis triple combination therapy has the advantage of combating drug resistance and side effects that limit the success of conventional cancer therapies.

CRediT authorship contribution statement

Bilgi Kip: Methodology, Investigation, Writing – original draft, Visualization. **Cansu Umran Tunc:** Investigation, Writing – original draft. **Omer Aydin:** Conceptualization, Supervision, Writing – review & editing, Project administration, Funding acquisition.

Declaration of competing interest

The authors declare that they have no known competing financial interests or personal relationships that could have appeared to influence the work reported in this paper.

Acknowledgment

This work was supported by Erciyes University Scientific Research Projects Coordination Unit under grant number FYL-2020-10657. C. U. Tunc recognizes the support of Erciyes University Scientific Research Projects Coordination Unit under grant number FDS-2020-9692. Bilgi Kip also recognizes the support of TUBITAK under project number 118C346.

The authors thank Ummugulsum Yilmaz (Department of Biomedical Engineering) for her guidance and support in the experimental designs. The figure was created with BioRender.com

References

[1] E. Dickens, S. Ahmed, Principles of cancer treatment by chemotherapy, Surgery (Oxford) 36 (2018) 134–138.
[2] R. Oun, Y.E. Moussa, N.J. Wheate, The side effects of platinum-based chemotherapy drugs: a review for chemists, Dalton Trans. 47 (19) (2018) 6645–6653.
[3] D.-W. Shen, L.M. Pouliot, M.D. Hall, M.M. Gottesman, Cisplatin resistance: a cellular self-defense mechanism resulting from multiple epigenetic and genetic changes, Pharmacol Rev 64 (2012) 706–721.
[4] W. Fan, B. Yung, P. Huang, X. Chen, Nanotechnology for multimodal synergistic cancer therapy, Chem. Rev. 117 (2017) 13566–13638.
[5] Y. Zhang, J. Yu, H.N. Bomba, Y. Zhu, Z. Gu, Mechanical force-triggered drug delivery, Chem. Rev. 116 (2016) 12536–12563.
[6] A.K. Wood, C.M. Sehgal, A review of low-intensity ultrasound for cancer therapy, Ultrasound Med Biol 41 (2015) 905–928.
[7] Y. Zhang, Y. Wan, Y. Chen, N.T. Blum, J. Lin, P. Huang, Ultrasound-Enhanced Chemo-Photodynamic Combination Therapy by Using Albumin "Nanoglue"-Based Nanotheranostics, ACS Nano 14 (2020) 5560–5569.
[8] S. Mullick Chowdhury, T. Lee, J.K. Willmann, Ultrasound-guided drug delivery in cancer, Ultrasonography 36 (2017) 171–184.
[9] X. Deng, Z. Shao, Y. Zhao, Solutions to the Drawbacks of Photothermal and Photodynamic Cancer Therapy, Adv. Sci. 8 (2021) 2002504.
[10] P. Decazes, P. Hinault, O. Veresezan, S. Thureau, P. Gouel, P. Vera, Trimodality PET/CT/MRI and Radiotherapy: A Mini-Review, Front Oncol 10 (2021).
[11] Z. Izadifar, P. Babyn, D. Chapman, Mechanical and biological effects of ultrasound: A review of present knowledge, Ultrasound Med. Biol. 43 (6) (2017) 1085–1104.
[12] Y. Meng, R.M. Reilly, R.C. Pezo, M. Trudeau, A. Sahgal, A. Singnurkar, J. Perry, S. Myrehaug, C.B. Pople, B. Davidson, M. Llinas, C. Hyen, Y. Huang, C. Hamani, S. Suppiah, K. Hynynen, N. Lipsman, MR-guided focused ultrasound enhances delivery of trastuzumab to Her2-positive brain metastases, Sci. Transl. Med. 13 (2021) eabj4011.
[13] O. Aydin, P. Chandran, R.R. Lorsung, G. Cohen, S.R. Burks, J.A. Frank, The Proteomic Effects of Pulsed Focused Ultrasound on Tumor Microenvironments of Murine Melanoma and Breast Cancer Models, Ultrasound Med. Biol. 45 (2019) 3232–3245.
[14] E. Vlaisavljevich, O. Aydin, K.-W. Lin, Y.Y. Durmaz, B. Fowlkes, M. ElSayed, Z. Xu, The role of positive and negative pressure on cavitation nucleation in nanodroplet-mediated histotripsy, Phys. Med. Biol. 61 (2015) 663.
[15] O. Aydin, E. Vlaisavljevich, Y. Yuksel Durmaz, Z. Xu, M.E.H. ElSayed, Noninvasive Ablation of Prostate Cancer Spheroids Using Acoustically-Activated Nanodroplets, Mol. Pharm. 13 (2016) 4054–4065.
[16] Y. Wu, X. Liu, Z. Qin, L. Hu, X. Wang, Low-frequency ultrasound enhances chemotherapy sensitivity and induces autophagy in PTX-resistant PC-3 cells via the endoplasmic reticulum stress-mediated PI3K/Akt/mTOR signaling pathway, OncoTargets and therapy 11 (2018) 5621.
[17] H. Li, H. Fan, Z. Wang, J. Zheng, W. Cao, T.W. Miller, Potentiation of Scutellarin on Human Tongue Carcinoma Xenograft by Low-Intensity Ultrasound, PLoS ONE 8 (3) (2013) e59473.
[18] V. Bernard, J. Škorpíková, V. Mornstein, I. Slaninová, Biological effects of combined ultrasound and cisplatin treatment on ovarian carcinoma cells, Ultrasonics 50 (2010) 357–362.
[19] R.G. Thomas, U.S. Jonnalagadda, J.J. Kwan, Biomedical Applications for Gas-Stabilizing Solid Cavitation Agents, Langmuir 35 (2019) 10106–10115.
[20] E. Vlaisavljevich, O. Aydin, Y.Y. Durmaz, K.-W. Lin, B. Fowlkes, Z. Xu, M.E. H. ElSayed, Effects of Droplet Composition on Nanodroplet-Mediated Histotripsy, Ultrasound Med. Biol. 42 (2016) 931–946.
[21] P. Zhang, J. He, X. Ma, J. Gong, Z. Nie, Ultrasound assisted interfacial synthesis of gold nanocones, Chem. Commun. 49 (2013) 987–989.
[22] P. Huang, P. Rong, J. Lin, W. Li, X. Yan, M.G. Zhang, L. Nie, G. Niu, J. Lu, W. Wang, X. Chen, Triphase Interface Synthesis of Plasmonic Gold Bellflowers as Near-Infrared Light Mediated Acoustic and Thermal Theranostics, JACS 136 (2014) 8307–8313.
[23] C. Mannaris, B.M. Teo, A. Seth, L. Bau, C. Coussios, E. Stride, Gas-Stabilizing Gold Nanocones for Acoustically Mediated Drug Delivery, Adv. Healthcare Mater. 7 (2018) 1800184.
[24] K. Präbst, H. Engelhardt, S. Ringgeler, H. Hübner, Basic colorimetric proliferation assays: MTT, WST, and resazurin, in: Cell viability assays, Springer, 2017, pp. 1-17.
[25] O. Aydin, I. Youssef, Y. Yuksel Durmaz, G. Tiruchinapally, M.E.H. ElSayed, Formulation of Acid-Sensitive Micelles for Delivery of Cabazitaxel into Prostate Cancer Cells, Mol. Pharm. 13 (2016) 1413–1429.
[26] H. Yan, X. Che, Q. Lv, L. Zhang, S. Dongol, Y. Wang, H. Sun, J. Jiang, Grifolin induces apoptosis and promotes cell cycle arrest in the A2780 human ovarian cancer cell line via inactivation of the ERK1/2 and Akt pathways, Oncology letters 13 (2017) 4806–4812.
[27] C.U. Tunç, D.Y. Öztaş, D. Uzunoğlu, Ö.F. Bayrak, M. Çulha, Silencing Breast Cancer Genes Using Morpholino Embedded DNA-Tile-AuNPs Nanostructures, Hum. Gene Ther. 30 (12) (2019) 1547–1558.
[28] R. Gupta, B. Rai, Effect of Size and Surface Charge of Gold Nanoparticles on their Skin Permeability: A Molecular Dynamics Study, Sci. Rep. 7 (2017) 45292.
[29] A. Verma, F. Stellacci, Effect of surface properties on nanoparticle-cell interactions, Small 6 (2010) 12–21.
[30] Y. Jia, W. Yuan, K. Zhang, J. Wang, P. Wang, Q. Liu, X. Wang, Comparison of cell membrane damage induced by the therapeutic ultrasound on human breast cancer MCF-7 and MCF-7/ADR cells, Ultrasonics Sonochemistry 26 (2015) 128–135.
[31] X. Xiong, R.R. Arvizo, S. Saha, D.J. Robertson, S. McMeekin, R. Bhattacharya, P. Mukherjee, Sensitization of ovarian cancer cells to cisplatin by gold nanoparticles, Oncotarget 5 (15) (2014) 6453–6465.
[32] N.A.P. Franken, H.M. Rodermond, J. Stap, J. Haveman, C. van Bree, Clonogenic assay of cells in vitro, Nat. Protoc. 1 (5) (2006) 2315–2319.

[33] B. Pandit, A.L. Gartel, J. Bauer, Thiazole antibiotic thiostrepton synergize with bortezomib to induce apoptosis in cancer cells, PloS One 6 (2) (2011) e17110.
[34] Y. Huai, Y. Zhang, X. Xiong, S. Das, R. Bhattacharya, P. Mukherjee, Gold Nanoparticles sensitize pancreatic cancer cells to gemcitabine, Cell Stress 3 (8) (2019) 267–279.
[35] C.J. Norbury, B. Zhivotovsky, DNA damage-induced apoptosis, Oncogene 23 (16) (2004) 2797–2808.
[36] D. Alimbetov, S. Askarova, B. Umbayev, T. Davis, D. Kipling, Pharmacological Targeting of Cell Cycle, Apoptotic and Cell Adhesion Signaling Pathways Implicated in Chemoresistance of Cancer Cells, Int. J. Mol. Sci. 19 (2018) 1690.
[37] S. Dasari, P.B. Tchounwou, Cisplatin in cancer therapy: molecular mechanisms of action, Eur J Pharmacol 740 (2014) 364–378.
[38] S.-H. Chen, J.-Y. Chang, New insights into mechanisms of cisplatin resistance: from tumor cell to microenvironment, Int. J. Mol. Sci. 20 (2019) 4136.
[39] S. Sharma, C. Santiskulvong, J. Rao, J.K. Gimzewski, O. Dorigo, The role of Rho GTPase in cell stiffness and cisplatin resistance in ovarian cancer cells, Integrative Biology: Quantitative Biosciences from nano to macro 6 (6) (2014) 611–617.
[40] G. Bassi, S. Panseri, S.M. Dozio, M. Sandri, E. Campodoni, M. Dapporto, S. Sprio, A. Tampieri, M. Montesi, Scaffold-based 3D cellular models mimicking the heterogeneity of osteosarcoma stem cell niche, Sci. Rep. 10 (2020) 22294.
[41] M. Chatzinikolaidou, Cell spheroids: the new frontiers in in vitro models for cancer drug validation, Drug Discovery Today 21 (9) (2016) 1553–1560.
[42] N. Niu, L. Wang, In vitro human cell line models to predict clinical response to anticancer drugs, Pharmacogenomics 16 (3) (2015) 273–285.
[43] S. Breslin, L. O'Driscoll, Three-dimensional cell culture: the missing link in drug discovery, Drug Discovery Today 18 (5-6) (2013) 240–249.
[44] D. Menshykau, Emerging technologies for prediction of drug candidate efficacy in the preclinical pipeline, Drug Discovery Today 22 (11) (2017) 1598–1603.
[45] R. Cairns, I. Papandreou, N. Denko, Overcoming physiologic barriers to cancer treatment by molecularly targeting the tumor microenvironment, Mol. Cancer Res. 4 (2) (2006) 61–70.
[46] A.L.B. Seynhaeve, M. Amin, D. Haemmerich, G.C. van Rhoon, T.L.M. ten Hagen, Hyperthermia and smart drug delivery systems for solid tumor therapy, Adv. Drug Deliv. Rev. 163-164 (2020) 125–144.
[47] C.-H. Heldin, K. Rubin, K. Pietras, A. Östman, High interstitial fluid pressure—an obstacle in cancer therapy, Nat. Rev. Cancer 4 (10) (2004) 806–813.
[48] Y. Matsumura, H. Maeda, A new concept for macromolecular therapeutics in cancer chemotherapy: mechanism of tumoritropic accumulation of proteins and the antitumor agent smancs, Cancer Res. 46 (1986) 6387–6392.
[49] Q. Zhang, H. Jin, L. Chen, Q. Chen, Y. He, Y. Yang, S. Ma, S. Xiao, F. Xi, Q. Luo, J. Liu, Effect of Ultrasound Combined With Microbubble Therapy on Interstitial Fluid Pressure and VX2 Tumor Structure in Rabbit, Front. Pharmacol. 10 (2019).